Statistical CSI-Based Distributed Precoding for Multi-Satellite Cooperative Transmission

Yafei Wang*†, Vu Nguyen Ha‡, Konstantinos Ntontin‡, Wenjin Wang*†,
Symeon Chatzinotas‡, and Björn Ottersten‡
*National Mobile Communications Research Laboratory, Southeast University, Nanjing 210096, China
†Purple Mountain Laboratories, Nanjing 211100, China
‡Interdisciplinary Centre for Security, Reliability and Trust (SnT), University of Luxembourg, Luxembourg.
Email: wangyf@seu.edu.cn, vu-nguyen.ha@uni.lu, kostantinos.ntontin@uni.lu, wangwj@seu.edu.cn,
{symeon.chatzinotas, bjorn.ottersten}@uni.lu

***Abstract*—This paper studies the distributed precoding design for multi-satellite massive MIMO transmission. We first conduct a detailed analysis of the transceiver process, examining the effects of delay and Doppler compensation errors and emphasizing the nearly independent nature of inter-satellite interference. Based on the derived signal model, an approximate expected sum rate maximization problem is formulated, incorporating statistical channel state information and compensation errors. Unlike conventional approaches that recast such problems as weighted minimum mean square error (WMMSE) minimization, we demonstrate that this transformation cannot hold equivalence in the considered scenario. To address this, we propose a modified WMMSE formulation leveraging channel covariance matrix decomposition. By exploiting channel characteristics, a low-complexity decomposition method is then developed, accompanied by an efficient algorithm. Simulation results validate the effectiveness and robustness of the proposed method in some practical simulated scenarios.**

I. Introduction

Satellite mobile communication has been anticipated to play a key role in the evolution of sixth-generation (6G) networks by enabling seamless global wireless connectivity [1]. In these networks, precoding serves as a fundamental technique to enhance spatial multiplexing capability within the same time-frequency resources [2]–[5]. However, the dynamic nature, long delays, and inherent characteristics of satellite communication (SatCom) environments pose significant challenges in acquiring channel state information (CSI), which leads to inevitable errors in the estimation of potential multipath components and the inter-satellite synchronization process. Therefore, precoding design based on statistical CSI (sCSI) merges as a more practical and feasible approach.

Most of the precoding studies in the literature have focused primarily on improving the capabilities of individual satellites. In [2], an MMSE-based precoding scheme was investigated under outdated CSI, while [3] and [4] proposed robust precoding designs to mitigate phase errors in CSI. For massive MIMO-enabled SatCom systems, [5] analyzed channel characteristics and developed a statistical CSI-based precoding mechanism to improve the average signal-to-leakage-plus-noise ratio (SLNR). In addition, [6] introduced novel techniques to reduce computational complexity in precoding updates. Given the limitations of single-satellite capacity due to link-budget constraints, deploying dense low Earth orbit (LEO) constellations with cooperative transmission has emerged as a promising solution. Recent advancements include cell-free LEO architectures [7], angle-based precoding for satellite swarms [8], and distributed MIMO performance evaluations [9]. In addition, hybrid precoding designs [10], coverage pattern analyses [11], multi-satellite spatial multiplexing [12], [13], and robust design to mitigate phase errors [14], [15] have further improved system performance. However, the key challenges such as delay and Doppler compensation under standard-compliant orthogonal frequency-division multiplexing (OFDM) modulation, as well as distributed precoding optimization, remain underexplored. Existing closed-form or heuristic designs have yet to fully investigate the performance limits in these critical aspects.

In this paper, we first analyse the transceiver process, examining the effects of delay and Doppler compensation errors and emphasizing the independence between inter-satellite interference. On this basis, we formulate an approximate expected sum rate maximization problem that considers both sCSI and compensation errors. While similar problems are often reformulated as weighted minimum mean square error (WMMSE) problems, it is demonstrated that this approach does not yield an equivalent solution in the considered scenario. Accordingly, we propose an equivalent modified WMMSE problem based on channel covariance matrix decomposition. By exploiting the channel characteristics, we develop a low-complexity decomposition method and propose an efficient solution algorithm.

II. System Model

Consider a downlink multi-satellite communication (mSatCom) system where S satellites serve K user terminals (UTs) over the same time-frequency resources. Each satellite is equipped with a uniform planar array (UPA) consisting of $N_{\mathrm{T}} = N_{\mathrm{v}} N_{\mathrm{h}}$ antennas, while each UT is equipped with a single antenna. As illustrated in Fig. 1, the master satellite, selected based on the highest service quality (e.g., the satellite nearest to the center of the cooperative transmission coverage area), cooperates with secondary satellites to transmit data using some cooperative mechanisms [16]. These satellites employ distributed precoding to serve the same terminals by coherently transmitting identical data. The *frequency-domain* channel

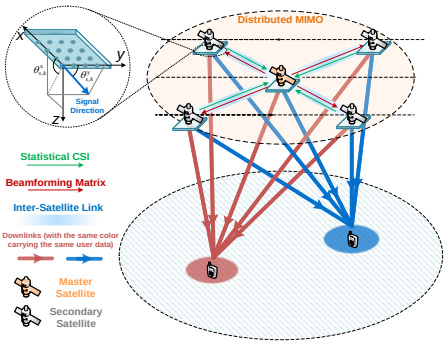

Fig. 1. Multi-satellite cooperative distributed precoding.

$\mathbf{h}_{s,k}(t,f) \in \mathbb{C}^{N_\mathrm{T}\times 1}$ from the s-th satellite to the k-th UT [5] can be written as

$$\mathbf{h}_{s,k}(t,f)=a_{s,k}(t,f)\mathrm{e}^{j2\pi(t\nu_{s,k}^{\mathrm{sat}}-f\tau_{s,k}^{\min})}\mathbf{v}(\boldsymbol{\theta}_{s,k}), \tag{1}$$

where $a_{s,k}(t,f)$ denotes the channel gain containing LoS and NLoS parts, following Rician fading distribution with the Rician factor $\kappa_{s,k}$ and power $\mathbb{E}_{t,f}\left[|a_{s,k}(t,f)|^2\right]=\gamma_{s,k}$ [5], [17], [18]; $\nu_{s,k}^{\mathrm{sat}}$ denotes the Doppler shift induced by satellite movement, and $\tau_{s,k}^{\min}$ corresponds to the propagation delay of the satellite-user LoS path; $\mathbf{v}(\boldsymbol{\theta}_{s,k}) \in \mathbb{C}^{N_\mathrm{T}\times 1}(\boldsymbol{\theta}_{s,k}=[\theta_{s,k}^{\mathrm{x}},\theta_{s,k}^{\mathrm{y}}]^T)$ is the steer vector given by

$$\mathbf{v}(\boldsymbol{\theta}_{s,k}) = \mathbf{v}_{N_\mathrm{v}}(\cos(\theta_{s,k}^{\mathrm{y}}))\otimes\mathbf{v}_{N_\mathrm{h}}(\sin(\theta_{s,k}^{\mathrm{y}})\cos(\theta_{s,k}^{\mathrm{x}})), \tag{2}$$

$$\mathbf{v}_N(x) = 1/\sqrt{N}\cdot[\mathrm{e}^{-j\pi 0x},\mathrm{e}^{-j\pi 1x},...,\mathrm{e}^{-j\pi(N-1)x}], \tag{3}$$

where $\theta_{s,k}^{\mathrm{x}}$ and $\theta_{s,k}^{\mathrm{y}}$ are the two departure angles of the signal with respect to the UPA, as shown in Fig. 1; $\mathbf{v}_{N_\mathrm{v}}$ and $\mathbf{v}_{N_\mathrm{h}}$ are formed from the general vector expression in (3), where N corresponds to N_v and N_h, respectively.

III. Received Signal Model and Rate Expression under Multi-Satellite Distributed Precoding

A. Imperfect Delay and Doppler Compensation

To enable coherent transmission across multiple satellites and ensure accurate OFDM demodulation at the receiver, the signal of each UT (or beam) must undergo independent OFDM modulation at the transmitter. The entire system bandwidth is utilized for OFDM transmission, where all users occupy the full set of subcarriers, and user scheduling is achieved through power allocation. Following the inverse Fourier transform (IFT), the baseband signal transmitted from satellite s to UT k over symbols $0,...,M-1$ is given by

$$\mathbf{x}_{s,k}(t)=\sum_{n=0}^{N-1}\sum_{m=0}^{M-1}\mathbf{x}_{s,k,n}^{(m)}\cdot u(t-mT_{\mathrm{sym}})\mathrm{e}^{j2\pi n\Delta f(t-mT_{\mathrm{sym}})}, \tag{4}$$

where $t\in(-\infty,\infty)$, $u(t)=\begin{cases}1, & t\in[0,T]\\ 0, & \text{others}\end{cases}$, N is the number of subcarriers, $T_{\mathrm{sym}}=T_{\mathrm{cp}}+T$ denotes the duration of a single OFDM symbol, T_{cp} is the cyclic prefix (CP) duration and T is the data duration. $\mathbf{x}_{s,k,n}^{(m)}$ is the precoded data at the n-th subcarrier of m-th OFDM symbol. Then, after adding CP and applying upconversion[1], we obtain the following bandpass transmit signal at the carrier frequency f_0:

$$\hat{\mathbf{x}}_{s,k}(t)=\begin{cases}\mathrm{e}^{j2\pi f_0 t}\mathbf{x}_{s,k}(t+T), & t\in[mT_{\mathrm{sym}}-T_{\mathrm{cp}},mT_{\mathrm{sym}}),\\ \mathrm{e}^{j2\pi f_0 t}\mathbf{x}_{s,k}(t), & t\in[mT_{\mathrm{sym}},mT_{\mathrm{sym}}+T),\end{cases} \tag{5}$$

Subsequently, delay and Doppler compensation are performed, and the transmit signal becomes

$$\hat{\mathbf{x}}_{s,k}^{\mathrm{cps}}(t)=\hat{\mathbf{x}}_{s,k}(t+\tau_{s,k}^{\mathrm{cps}})\cdot\mathrm{e}^{-j2\pi(t+\tau_{s,k}^{\mathrm{cps}})\nu_{s,k}^{\mathrm{cps}}}, \tag{6}$$

where $\tau_{s,k}^{\mathrm{cps}}$ and $\nu_{s,k}^{\mathrm{cps}}$ represent the *delay and Doppler compensation values* of the s-th satellite for the k-th UT. Then, the bandpass received signal is obtained by convolving the *delay-domain* channel (obtained by applying the inverse Fourier transform to the *frequency-domain* channel) with the transmit signal, expressed as

$$y_{s,k}(t)=\sum_{\forall(l,s)}\breve{\mathbf{h}}_{s,k}^T\hat{\mathbf{x}}_{s,l}(t+\tau_{s,l}^{\mathrm{cps}}-\tau_{s,k}^{\min}) \cdot\mathrm{e}^{j2\pi t(\nu_{s,k}^{\mathrm{sat}}-\nu_{l,k}^{\mathrm{cps}})}\mathrm{e}^{-j2\pi(\tau_{s,l}^{\mathrm{cps}}-\tau_{s,k}^{\min})\nu_{s,l}^{\mathrm{cps}}}, \tag{7}$$

where $\breve{\mathbf{h}}_{s,k}\triangleq a_{s,k}(t,\tau_{s,k}^{\min})\mathbf{v}(\boldsymbol{\theta}_{s,k})$. We define the delay and Doppler compensation errors, as well as their impact on interference to other UTs, as follows:

$$\bar{\tau}_{s,k}\triangleq\tau_{s,k}^{\mathrm{cps}}-\tau_{s,k}^{\min},\ \bar{\nu}_{s,k}\triangleq\nu_{s,k}^{\mathrm{sat}}-\nu_{s,k}^{\mathrm{cps}}, \tag{8}$$

$$\tilde{\tau}_{s,l,k}\triangleq\tau_{s,l}^{\mathrm{cps}}-\tau_{s,k}^{\min},\ \tilde{\nu}_{s,l,k}\triangleq\nu_{s,k}^{\mathrm{sat}}-\nu_{s,l}^{\mathrm{cps}}. \tag{9}$$

At the receiver, the time-domain baseband signal of the m-th OFDM symbol is $y_{s,k}^{(m)}(t)=y_{s,k}(t)\hat{u}(t-mT_{\mathrm{sym}})$, where $\hat{u}(t)=1$ if $t\in[-T_{\mathrm{cp}},T]$ and $\hat{u}(t)=0$, otherwise.

B. Received Signal Model and New Features

For the k-th UT, the effective signal from the s-th satellite is given by $\breve{\mathbf{h}}_{s,k}^T\hat{\mathbf{x}}_{s,k}(t+\bar{\tau}_{s,k})\cdot\mathrm{e}^{j2\pi(t\bar{\nu}_{s,k}-\bar{\tau}_{s,k}\nu_{s,k}^{\mathrm{cps}})}$. Here, the parameter $\bar{\tau}_{s,k}$ determines whether inter-symbol interference (ISI) is introduced. If the first sample of the effective signal after delay compensation falls within the transmit symbol's CP, no ISI is introduced; otherwise, ISI will occur. Here, we assume the former case. After downconversion, sampling, CP removal, and DFT, the received signal at the n-th subcarrier is expressed as:

$$\begin{aligned}y_{k,n}^{\mathrm{eff}(m)}&=\sum_{\forall s}\breve{\mathbf{h}}_{s,k}^T\sum_{n'=0}^{N-1}\varphi_{s,k}^{n'}\mathbf{x}_{s,k,n'}^{(m)}\psi(\bar{\nu}_{s,k},n'-n),\\ &\overset{(a)}{\approx}\sum_{\forall s}\breve{\mathbf{h}}_{s,k}^T\,\mathbf{x}_{s,k,n}^{(m)}\varphi_{s,k}^{n},\end{aligned} \tag{10}$$

where $\varphi_{s,k}^{n}=\mathrm{e}^{j2\pi(f_0+n\Delta f-\nu_{s,k}^{\mathrm{cps}})\bar{\tau}_{s,k}}$, $\psi(\bar{\nu}_{s,k},n'-n)=\frac{1}{N}\frac{1-\mathrm{e}^{j2\pi\left[\bar{\nu}_{s,k}/\Delta f-(n'-n)\right]}}{1-\mathrm{e}^{j2\pi\left[\bar{\nu}_{s,k}/\Delta f-(n'-n)\right]/N}}$ characterizes the inter-carrier interference (ICI) introduced by Doppler estimation error $\bar{\nu}_{s,k}$, $\Delta f=\frac{1}{T}$ is the subcarrier spacing, and approximation (a) is obtained under the assumption that $\bar{\nu}_{s,k}\ll\Delta f$.

The interference signal from the s-th satellite and the l-th ($l\neq k$) UT is $\breve{\mathbf{h}}_{s,k}^T\hat{\mathbf{x}}_{s,l}(t+\tilde{\tau}_{s,l,k})\cdot\mathrm{e}^{j2\pi(t\bar{\nu}_{s,l,k}-\tilde{\tau}_{s,l,k}\nu_{s,l}^{\mathrm{cps}})}$. For

[1]In this paper, upconversion is performed prior to delay compensation; however, in practical systems, the sequence of these operations may vary without impacting the final analysis results.

simplicity, we represent the interference signal after Downconversion, sampling, CP removal, and DFT as

$$y_{k,n}^{\mathrm{interf}(m)} \approx \sum_{\forall s}\sum_{\forall l\neq k} \breve{\mathbf{h}}_{s,k}^{T}\, \breve{\mathbf{x}}_{s,l,n}^{(m'_{s,l,k})} \varphi_{s,l,k}^{n}, \tag{11}$$

where $\varphi_{s,l,k}^{n} = \mathrm{e}^{j2\pi(f_0+n\Delta f-\nu_{s,l}^{\mathrm{cps}})\tilde{\nu}_{s,l,k}}$.

Remark 1. *The interference signal model is characterized by the following key points:*

1) ***ISI&ICI:*** *The interference signal may contain much ISI and ICI due to the potentially large values of $|\tilde{\tau}_{s,l,k}|$ and $|\tilde{\nu}_{s,l,k}|$, which means $\breve{\mathbf{x}}_{s,l,n}^{(m'_{s,l,k})}$ may contain signals from multiple OFDM symbols and multiple subcarriers $\mathbf{x}_{s,l,1}^{(m'_{s,l,k})},\ldots,\mathbf{x}_{s,l,N}^{(m'_{s,l,k})}$.*
2) ***Inter-satellite interference independence:*** *For the two interference signals at UT k caused by the signals for UT l transmitted by satellites s_1 and s_2, when $\Delta\tau_{l,k}^{s_1,s_2} = |(\tau_{s_1,l}^{\min}-\tau_{s_1,k}^{\min})-(\tau_{s_2,l}^{\min}-\tau_{s_2,k}^{\min})| \approx |\tilde{\tau}_{s_1,l,k}-\tilde{\tau}_{s_2,l,k}| > T_{\mathrm{sym}}$, the symbols corresponding to indices $m'_{s_1,l,k}$ and $m'_{s_2,l,k}$ become independent, resulting in the two interference signals being uncorrelated. Due to the large distances between different satellites on the same or different orbital planes, $\Delta\tau_{l,k}^{s_1,s_2}$ tends to be generally large, whereas T_{sym} remains relatively small, making this scenario highly probable. With satellites at an altitude of 600 km serving UTs uniformly distributed within an 800 km radius area below, the probability of $\Delta\tau_{l,k}^{s_1,s_2} > T$ is shown in Fig. 2. Since the proportion of T_{cp} is small, its impact on the conclusion is minimal. Moreover, when user scheduling is taken into account [19], [20], the user distribution may become more dispersed, further increasing the probability.*

Since we consider designing the precoding based on statistical CSI, such scheme remains unchanged over multiple consecutive symbols. Besides, we ignore the subcarrier index for simplicity. Thus, the received signal on the m-th OFDM symbol for UT k can be expressed as

$$y_k^{(m)} = \sum_{\forall s}\breve{\mathbf{h}}_{s,k}^{T}\left(\mathbf{w}_{s,k}d_k^{(m)}\varphi_{s,k} + \sum_{\forall l\neq k}\mathbf{w}_{s,l}\breve{d}_l^{(m'_{s,l,k})}\varphi_{s,l,k}\right) + n_k^{(m)} \tag{12}$$

where $d_k^{(m)}$ represents the symbol information for the k-th UT at m-th OFDM symbol, and $n_k^{(m)} \sim \mathcal{CN}(0,\sigma_k^2)$ denotes the additive noise at the k-th UT. $\varphi_{s,k}$ is the phase error introduced by delay and Doppler estimation errors. In practical satellite systems, Doppler shift and delay should be estimated at the UT based on pilots in the downlink [21]. The estimated parameters are then fed back to the satellite, where the variations during the feedback process are further predicted, followed by precompensation. Thus, the distribution of $\varphi_{s,k}$ depends on the overall estimation scheme.

C. Sum Rate Expression and Statistical CSI Exploitation

We assume that the information of different UTs is independent, $\mathbb{E}\{d_k^{(m)}(d_k^{(m)})^H\}=1$, and $\mathbb{E}\{\breve{d}_l^{(m'_{s,l,k})}(\breve{d}_l^{(m'_{s,l,k})})^H\}=1$. Due to the independence of inter-satellite interference, we approximate $\mathbb{E}\{\breve{d}_{s_1,l}^{(m'_{s_1,l,k})}(\breve{d}_{s_2,l}^{(m'_{s_2,l,k})})^H\} \approx 0$. Based on the above analysis, the expected achievable rate is given by

$$\begin{aligned}\mathbb{E}\{R_k\} &= \mathbb{E}_{\mathbf{H}}\left\{\log_2\left(1+\frac{\sum_{s_1=1}^{S}\sum_{s_2=1}^{S}\mathbf{w}_{s_1,k}^H\bar{\mathbf{h}}_{s_1,k}^*\bar{\mathbf{h}}_{s_2,k}^T\mathbf{w}_{s_2,k}}{\sum_{i\neq k}\sum_{s=1}^{S}\mathbf{w}_{s,i}^H\bar{\mathbf{h}}_{s,k}^*\bar{\mathbf{h}}_{s,k}^T\mathbf{w}_{s,i}+\sigma_k^2}\right)\right\}\\ &\approx \bar{R}_k \triangleq \log_2\left(1+\frac{\sum_{s_1=1}^{S}\sum_{s_2=1}^{S}\mathbf{w}_{s_1,k}^H\mathbb{E}\{\bar{\mathbf{h}}_{s_1,k}^*\bar{\mathbf{h}}_{s_2,k}^T\}\mathbf{w}_{s_2,k}}{\sum_{i\neq k}\sum_{s=1}^{S}\mathbf{w}_{s,i}^H\mathbb{E}\{\bar{\mathbf{h}}_{s,k}^*\bar{\mathbf{h}}_{s,k}^T\}\mathbf{w}_{s,i}+\sigma_k^2}\right),\end{aligned}$$

where $\bar{\mathbf{h}}_{s,k} = \breve{\mathbf{h}}_{s,k}\varphi_{s,k}$. The expression can be rewritten as

$$\bar{R}_k = \log_2\left(1+\frac{\mathbf{w}_k^H\boldsymbol{\Omega}_k\mathbf{w}_k}{\sum_{i\neq k}\mathbf{w}_i^H\tilde{\boldsymbol{\Omega}}_k\mathbf{w}_i+\sigma_k^2}\right), \tag{13}$$

in which

$$\mathbf{w}_k = [\mathbf{w}_{1,k}^T,\mathbf{w}_{2,k}^T,\cdots,\mathbf{w}_{S,k}^T]^T \in \mathbb{C}^{SN_{\mathrm{T}}\times 1}, \tag{14}$$

$$\bar{\mathbf{h}}_k = [\bar{\mathbf{h}}_{1,k}^T,\bar{\mathbf{h}}_{2,k}^T,\cdots,\bar{\mathbf{h}}_{S,k}^T]^H \in \mathbb{C}^{SN_{\mathrm{T}}\times 1}, \tag{15}$$

$$\boldsymbol{\Omega}_{s1|s2,k} = \mathbb{E}\{\bar{\mathbf{h}}_{s_1,k}^*\bar{\mathbf{h}}_{s_2,k}^T\},\ \boldsymbol{\Omega}_k = \mathbb{E}[\bar{\mathbf{h}}_k^*\bar{\mathbf{h}}_k^T], \tag{16}$$

$$\tilde{\boldsymbol{\Omega}}_k = \mathrm{blkdiag}\{\boldsymbol{\Omega}_{1|1,k},...,\boldsymbol{\Omega}_{S|S,k}\} \in \mathbb{C}^{SN_{\mathrm{T}}\times SN_{\mathrm{T}}}. \tag{17}$$

According to the channel model given in Section II, one yields

$$\mathbb{E}\{\bar{\mathbf{h}}_{s,k}\} = \rho_{s,k}\cdot\mathbf{v}(\theta_{s,k}^{\mathrm{x}},\theta_{s,k}^{\mathrm{y}}), \tag{18}$$

$$\boldsymbol{\Omega}_{s1|s2,k} = \begin{cases}\gamma_{s,k}\mathbf{v}^*(\boldsymbol{\theta}_{s,k})\mathbf{v}^T(\boldsymbol{\theta}_{s,k}),\ s_1=s_2=s,\\ \rho_{s_1,k}^*\rho_{s_2,k}\mathbf{v}^*(\boldsymbol{\theta}_{s_1,k})\mathbf{v}^T(\boldsymbol{\theta}_{s_2,k}),\ s_1\neq s_2,\end{cases} \tag{19}$$

$$\rho_{s,k} = \sqrt{\frac{\kappa_{s,k}\gamma_{s,k}}{2(\kappa_{s,k}+1)}}\cdot(1+j)\cdot\bar{\varphi}_{s,k}, \tag{20}$$

where $\gamma_{s,k}$, $\kappa_{s,k}$, $\boldsymbol{\theta}_{s,k}$, and $\bar{\varphi}_{s,k} \triangleq \mathbb{E}\{\varphi_{s,k}\}$ represent the average channel power, K-factor, the angle from the transmit antenna array to the UT, and the expectation of the phase error, respectively. We refer to these parameters as statistical CSI, and assume that they remain constant over a long duration and can be accurately estimated [4], [5].

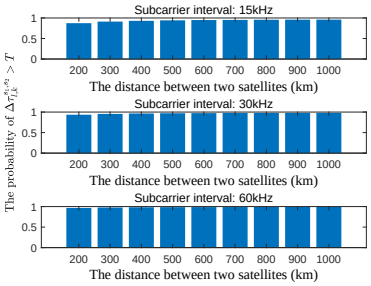

Fig. 2. Probability of independent inter-satellite interference.

IV. Statistical Distributed Precoding Design

Without loss of generality, we consider per-subcarrier power constraints [22], and the weighted sum rate (WSR) maximization problem can be stated as

$$(\mathcal{P}_1):\ \max_{\mathbf{W}}\ \sum_{\forall k}\beta_k\bar{R}_k \text{ s.t. } \mathrm{Tr}\left(\mathbf{W}_s\mathbf{W}_s^H\right)\leq P_s,\ s\in\mathcal{S}, \tag{21}$$

where β_k is the weight of the k-th UT's rate, and P_s is the maximum transmit power of s-th satellite on the considered subcarrier. Unlike the problems in existing literatures, since the expression for $\bar{R}_k$ is a unique formulation based on the system model and statistical CSI in Section III, the proposed problem $(\mathcal{P}_1)$ is a novel optimization problem. Besides, the model in

Section III also applies to other classical criteria for precoding design [23]–[25].

A. WSR Criterion vs. WMMSE Criterion

Similar to the process of solving the WSR problem in previous references [14] and [15], a straightforward approach is solving the following expected MSE optimization problem

$$\begin{aligned}(\mathcal{P}_2): \quad &\min_{\mathbf{W},\mathbf{a},\mathbf{u}} \sum_{\forall k}\beta_k\left(u_k e_k - \log_2(u_k)\right)\\ &\text{s.t. } \mathrm{Tr}\left(\mathbf{W}_s\mathbf{W}_s^H\right) \le P_s,\ s\in\mathcal{S}.\end{aligned} \tag{22}$$

where $\mathbf{a} \in \mathbb{C}^{K\times 1}$ and $\mathbf{u} \in \mathbb{C}^{K\times 1}$ are auxiliary parameters, which can be interpreted as receiver and weight for the expected mean squared error (MSE), respectively. $e_k = \mathbb{E}_{\mathbf{H},\mathbf{d},n_k}\left[|\hat{d}_k^{(m)} - d_k^{(m)}|^2\right]$ represents the MSE between the signal to be demodulated and the information symbol of the k-th UT, which is expressed as:

$$\begin{aligned}e_k = a_k a_k^H\Big(\sum_{\forall i\neq k}\mathbf{w}_i^H\tilde{\mathbf{\Omega}}_k\mathbf{w}_i + \mathbf{w}_k^H\mathbf{\Omega}_k\mathbf{w}_k\Big) - a_k^H\mathbb{E}\{\bar{\mathbf{h}}_k^T\}\mathbf{w}_k\\ - a_k\mathbf{w}_k^H\mathbb{E}\{\bar{\mathbf{h}}_k^*\} + a_k a_k^H\sigma_k^2 + 1.\end{aligned} \tag{23}$$

Proposition 1. *In the sense that the optimal* $\mathbf{W}$ *is identical, the WSR problem* ($\mathcal{P}_1$) *and the WMMSE problem* ($\mathcal{P}_2$) *are not equivalent when*

$$\mathbb{E}\{\bar{\mathbf{h}}_{s,k}^*\bar{\mathbf{h}}_{s,k}^T\} \neq \mathbb{E}\{\bar{\mathbf{h}}_{s,k}^*\}\mathbb{E}\{\bar{\mathbf{h}}_{s,k}^T\},\ \forall s\in\mathcal{S}, k\in\mathcal{K}. \tag{24}$$

Proof. *See Appendix A.*

According to the description of statistical CSI exploitation in Section III-C, we have

$$\frac{[\mathbb{E}\{\bar{\mathbf{h}}_{s,k}^*\bar{\mathbf{h}}_{s,k}^T\}]_{i,j}}{[\mathbb{E}\{\bar{\mathbf{h}}_{s,k}^*\}\mathbb{E}\{\bar{\mathbf{h}}_{s,k}^T\}]_{i,j}} = \frac{\kappa_{s,k}+1}{\kappa_{s,k}}\cdot\frac{1}{|\bar{\varphi}_{s,k}|^2},\ \forall i,j. \tag{25}$$

Since $|\bar{\varphi}_{s,k}|^2 = \mathbb{E}\{|\varphi_{s,k}|^2\} - \mathrm{var}(\varphi_{s,k}) = 1 - \mathrm{var}(\varphi_{s,k})$, we arrive at the following conclusion:

Remark 2. *When the LoS path dominates the satellite channel and the variance of the phase error is nearly zero, i.e.,* $\kappa_{s,k}\to\infty$ *and* $\mathrm{var}(\varphi_{s,k})\to 0$*, optimization problem* (22) *is nearly equivalent to optimization problem* (21)*. Conversely, the greater the deviation between the two.*

The above non-equivalence causes CSI errors to underestimate the effective signal power in the SINR expression, thus deviating from the WSR problem objective. To the best of our knowledge, due to multiple satellite power constraints and the novel channel characteristics of multi-satellite distributed precoding, existing robust WMMSE variants cannot be directly applied to this problem, which calls for the formulation of a new equivalent problem.

B. Modified WMMSE Criterion

By analyzing (23) and ($\mathcal{P}_1$)'s objective function, we formulate the following modified WMMSE (MWMMSE) problem:

$$\begin{aligned}(\mathcal{P}_3): \quad &\min_{\mathbf{W},\mathbf{A},\mathbf{u}} \sum_{\forall k}\beta_k\left(u_k\tilde{e}_k - \log_2(u_k)\right)\\ &\text{s.t. } \mathrm{Tr}\left(\mathbf{W}_s\mathbf{W}_s^H\right) \le P_s,\ s\in\mathcal{S}.\end{aligned} \tag{26}$$

where $\tilde{e}_k$ denotes the modified MSE error, expressed as

$$\begin{aligned}\tilde{e}_k = \mathbf{a}_k^H\mathbf{a}_k\Big(\sum_{\forall i\neq k}\mathbf{w}_i^H\tilde{\mathbf{\Omega}}_k\mathbf{w}_i + \mathbf{w}_k^H\mathbf{\Omega}_k\mathbf{w}_k\Big)\\ - \mathbf{a}_k^H\mathbf{Q}_k\mathbf{w}_k - \mathbf{w}_k^H\mathbf{Q}_k^H\mathbf{a}_k + \mathbf{a}_k^H\mathbf{a}_k\sigma_k^2 + 1,\end{aligned} \tag{27}$$

where vector $\mathbf{Q}_k$ is constructed to satisfy $\mathbf{\Omega}_k = \mathbf{Q}_k^H\mathbf{Q}_k$, and $\mathbf{a}_k$ can be regarded as a virtual receiver.

Proposition 2. *The WSR problem* ($\mathcal{P}_1$) *and the MWMMSE problem* ($\mathcal{P}_3$) *are equivalent in the sense that the optimal* $\mathbf{W}$ *is identical.*

Proof. *The proof is similar to Appendix A and is omitted here.*

Under perfect CSI, the MSE in (23) equivalently transforms the original objective function into a quadratic function with respect to $\mathbf{W}$; under the statistical CSI constructed in Section III, our proposed (27) achieves this equivalent transformation.

Remark 3. *The conventional MSE in* (23) *is a special case of the modified MSE* (27)*. When the perfect CSI is available,* $\mathbb{E}\{\bar{\mathbf{h}}_k^T\} = \bar{\mathbf{h}}_k^T$ *and* $\mathbf{\Omega}_k = \bar{\mathbf{h}}_k^*\bar{\mathbf{h}}_k^T$*, and hence* (27) *degenerates into* (23)*.*

C. Low-Complexity Covariance Matrix Decomposition

$\mathbf{\Omega}_k$ is a Hermitian matrix and can be decomposed via some methods like Cholesky decomposition. However, this introduces computational complexity of $\mathcal{O}\left(S^3N_{\mathrm{T}}^3\right)$, and the resulting dimension $SN_{\mathrm{T}}\times SN_{\mathrm{T}}$ of $\mathbf{Q}_k$ leads to higher complexity for subsequent optimization. Fortunately, based on the analysis in Sections II and III-C, the channel in multi-satellite cooperative transmission exhibits unique statistical properties, which allow the following decomposition to hold:

$$\mathbf{\Omega}_k = \mathbf{Q}_k^H\mathbf{Q}_k,\ \mathbf{Q}_k = \begin{bmatrix}\mathbb{E}\{\bar{\mathbf{h}}_k^T\}\\ \bar{\mathbf{Q}}_k\end{bmatrix} \in \mathbb{C}^{(S+1)\times SN_{\mathrm{T}}}, \tag{28}$$

$$\bar{\mathbf{Q}}_k = \mathrm{blkdiag}\{\varkappa_{1,k}\bar{\mathbf{h}}_{1,k}^T, ..., \varkappa_{S,k}\bar{\mathbf{h}}_{S,k}^T\}, \tag{29}$$

where $\varkappa_{s,k} = \sqrt{\frac{\gamma_{s,k}-\rho_{s,k}^*\rho_{s,k}}{\rho_{s,k}^*\rho_{s,k}}}$. This decomposition does not introduce additional computational complexity, and the number of rows in $\mathbf{Q}_k$ is much smaller than that of its columns, i.e., $S+1 \ll SN_{\mathrm{T}}$, which reduces the complexity of subsequent calculations. Furthermore, to simplify and reduce the complexity of the $\mathbf{w}_i^H\tilde{\mathbf{\Omega}}_k\mathbf{w}_i$ term in subsequent calculations, we further decompose $\tilde{\mathbf{\Omega}}_k$ as $\tilde{\mathbf{\Omega}}_k = \tilde{\mathbf{Q}}_k^H\tilde{\mathbf{Q}}_k$, and $\tilde{\mathbf{Q}} \in \mathbb{C}^{S\times SN_{\mathrm{T}}}$ is given by

$$\tilde{\mathbf{Q}}_k = \mathrm{blkdiag}\{\tilde{\varkappa}_{1,k}\bar{\mathbf{h}}_{1,k}^T, ..., \tilde{\varkappa}_{S,k}\bar{\mathbf{h}}_{S,k}^T\}, \tag{30}$$

where $\tilde{\varkappa}_{s,k} = \sqrt{\frac{\gamma_{s,k}}{\rho_{s,k}^*\rho_{s,k}}}$. Under the above decomposition, the dimension of virtual receiver is $\mathbf{A} = [\mathbf{a}_1, ..., \mathbf{a}_K] \in \mathbb{C}^{(S+1)\times K}$.

D. Robust Multi-Satellite Distributed Preccoding Design

Due to individual satellite power constraints, the problem deviates from the single-satellite case, where solution derivation is more tractable. An effective approach is presented in [14], [15], which reformulates the satellite power constraints into per-user constraints. However, this work focuses on WMMSE

$$f(\mathbf{W},\boldsymbol{\eta}) = \sum_{k=1}^{K} \beta_k u_k \left[\frac{\mathbf{a}_k^H \mathbf{a}_k}{\eta_k^2} \left(\sum_{i \neq k} \mathbf{w}_i^H \tilde{\boldsymbol{\Omega}}_k \mathbf{w}_i + \mathbf{w}_k^H \boldsymbol{\Omega}_k \mathbf{w}_k \right) - \frac{\mathbf{a}_k^H \mathbf{Q}_k \mathbf{w}_k}{\eta_k} - \frac{\mathbf{w}_k^H \mathbf{Q}_k^H \mathbf{a}_k}{\eta_k} + \frac{\mathbf{a}_k^H \mathbf{a}_k \sigma_k^2}{\eta_k^2} \right]. \tag{34}$$

$$\tilde{f}(\mathbf{W},\boldsymbol{\eta}) = \sum_{k=1}^{K} \beta_k u_k \left[\mathbf{a}_k^H \mathbf{a}_k \left(\sum_{i \neq k} \frac{\mathbf{w}_i^H \tilde{\boldsymbol{\Omega}}_k \mathbf{w}_i}{\eta_i^2} + \frac{\mathbf{w}_k^H \boldsymbol{\Omega}_k \mathbf{w}_k}{\eta_k^2} \right) - \frac{\mathbf{a}_k^H \mathbf{Q}_k \mathbf{w}_k}{\eta_k} - \frac{\mathbf{w}_k^H \mathbf{Q}_k^H \mathbf{a}_k}{\eta_k} + \frac{\mathbf{a}_k^H \mathbf{a}_k \sigma_k^2}{\eta_k^2} \right]. \tag{35}$$

criterion and ignores some interference terms and renders the treatment of power constraints ambiguous. For our formulated problem (26), we also transform its constraints into per-user power constraints and present a mathematically rigorous and accurate solution process. Problem $(\mathcal{P}_3)$ is reformulated as follows:

$$\begin{aligned} (\mathcal{P}_4): \quad & \min_{\mathbf{W},\mathbf{A},\mathbf{u}} \sum_{\forall k} \beta_k \left(u_k \tilde{e}_k - \log_2(u_k) \right) \\ & \text{s.t. } \mathrm{Tr}\left(\mathbf{w}_k \mathbf{w}_k^H \right) = P_k, \ k \in \mathcal{K}. \end{aligned} \tag{31}$$

where, to simplify the problem solving, we consider an equality power constraint. To address this problem, alternate optimization approaches proposed in [26], [27] can be adopted as follows.

1) Optimizing $\mathbf{A}$ *and* $\mathbf{u}$*:* When $\mathbf{W}$ and $\mathbf{u}$ are fixed, the optimal $\mathbf{A}$ can be obtained by taking the derivative of the objective function, given by:

$$\mathbf{a}_k^\star = \frac{\mathbf{Q}_k \mathbf{w}_k}{\mathbf{w}_k^H \boldsymbol{\Omega}_k \mathbf{w}_k + \sum_{\forall i \neq k} \mathbf{w}_i^H \tilde{\boldsymbol{\Omega}}_k \mathbf{w}_i + \sigma_k^2}. \tag{32}$$

Furthermore, when $\mathbf{W}$ and $\mathbf{A}$ are fixed, the optimal $\mathbf{u}$ is given by $u_k^\star = \tilde{e}_k^{-1}$.

2) Optimizing $\mathbf{W}$*:* Given $\mathbf{A}$ and $\mathbf{u}$, solving $(\mathcal{P}_4)$ becomes slightly more challenging. Following [26], we introduce a scaling factor η_k for each $\mathbf{a}_k$ to further optimize. This essentially corresponds to a joint optimization of $\mathbf{W}$ and scaling of $\mathbf{a}$. Then, the problem becomes

$$\min_{\mathbf{W},\boldsymbol{\eta}} \ f(\mathbf{W},\boldsymbol{\eta}) \qquad \text{s.t. } \mathrm{Tr}\left(\mathbf{w}_k \mathbf{w}_k^H \right) \leq P_k, \ k \in \mathcal{K}. \tag{33}$$

where the expression of $f(\mathbf{W},\boldsymbol{\eta})$ is (34). Considering that SatCom systems are not interference-limited, meaning that the interference is relatively small compared to the effective signal and noise, we approximate $f(\mathbf{W},\boldsymbol{\eta})$ using the function $\tilde{f}(\mathbf{W},\boldsymbol{\eta})$, as shown in (35). This approximation decouples the optimization of $\mathbf{w}_k$ and η_k for each UT, transforming the optimization problem into:

$$\begin{aligned} \min_{\mathbf{w}_k,\eta_k} \ & \frac{\mathbf{w}_k^H \boldsymbol{\Xi}_k \mathbf{w}_k + \mathbf{a}_k^H \mathbf{a}_k \sigma_k^2}{\eta_k^2} - \frac{\beta_k u_k}{\eta_k} \left(\mathbf{a}_k^H \mathbf{Q}_k \mathbf{w}_k + \mathbf{w}_k^H \mathbf{Q}_k^H \mathbf{a}_k \right) \\ & \text{s.t. } \mathrm{Tr}\left(\mathbf{w}_k \mathbf{w}_k^H \right) = P_k, \end{aligned} \tag{36}$$

where $\boldsymbol{\Xi}_k = \beta_k u_k (\mathbf{a}_k^H \mathbf{a}_k) \boldsymbol{\Omega}_k + \sum_{\forall i \neq k} \beta_i u_i (\mathbf{a}_i^H \mathbf{a}_i) \tilde{\boldsymbol{\Omega}}_i$.

Proposition 3. *The following expressions of* $\mathbf{w}_k$ *and* η_k *achieve the optimality of optimization problem* (36)*.*

$$\mathbf{w}_k^\star = \eta_k^\star (\boldsymbol{\Xi}_k + \frac{\beta_k u_k \mathbf{a}_k^H \mathbf{a}_k \sigma_k^2}{P_k} \mathbf{I})^{-1} \beta_k u_k \mathbf{Q}_k^H \mathbf{a}_k, \tag{37}$$

$$\eta_k^\star = \sqrt{P_k / \| (\boldsymbol{\Xi}_k + \tfrac{\beta_k u_k \mathbf{a}_k^H \mathbf{a}_k \sigma_k^2}{P_k} \mathbf{I})^{-1} \beta_k u_k \mathbf{Q}_k^H \mathbf{a}_k \|_2^2}. \tag{38}$$

Proof. *The proof is similar to that in [28] and is omitted here.*

Algorithm 1 MS-JoMWMMSE Algorithm for Problem (26)

1: **Input:** $\{\gamma_{s,k}, \kappa_{s,k}, \boldsymbol{\theta}_{s,k}, \bar{\varphi}_{s,k}\}_{\forall s,k}$, $\{P_s\}_{\forall s}$, $\{\sigma_k^2, \beta_k\}_{\forall k}$, $I_{\max}$.
2: Construct $\{\mathbf{Q}_k, \tilde{\mathbf{Q}}_k\}_{\forall k}$ using (28), (29), (18), (30).
3: Initialize $\{\mathbf{W}_s\}_{\forall s}$. $n = 0$.
4: Initialize $P_k = (\sum_{s \in \mathcal{S}} P_s)/K$, $\tilde{e}_k = \chi$, $\tilde{e}'_k = \infty$, $\forall k \in \mathcal{K}$.
5: **while** $n < I_{\max}$ **and** $\sum_{k=1}^{K} \log_2(\tilde{e}'_k / \tilde{e}_k) > \chi$ **do**
6: $n = n + 1$. $\tilde{e}'_k = \tilde{e}_k$.
7: $\mathbf{a}_k = \frac{\mathbf{Q}_k \mathbf{w}_k}{\left(\sum_{i \neq k} \mathbf{w}_i^H \tilde{\boldsymbol{\Omega}}_k \mathbf{w}_i + \mathbf{w}_k^H \boldsymbol{\Omega}_k \mathbf{w}_k \right) + \sigma_k^2}$, $\forall k \in \mathcal{K}$.
8: Compute $\tilde{e}_k$ with (27), $u_k = \tilde{e}_k^{-1}$, $\forall k \in \mathcal{K}$.
9: $\boldsymbol{\Xi}_k = \beta_k u_k (\mathbf{a}_k^H \mathbf{a}_k) \boldsymbol{\Omega}_k + \sum_{i=1, i \neq k}^{K} \beta_i u_i (\mathbf{a}_i^H \mathbf{a}_i) \tilde{\boldsymbol{\Omega}}_i$, $\forall k \in \mathcal{K}$.
10: $\bar{\mathbf{w}}_k = \left(\boldsymbol{\Xi}_k + \frac{\beta_k u_k \mathbf{a}_k^H \mathbf{a}_k \sigma_k^2}{P_k} \mathbf{I} \right)^{-1} \beta_k u_k \mathbf{Q}_k^H \mathbf{a}_k$, $\forall k \in \mathcal{K}$.
11: $\eta_k = \sqrt{\frac{P_k}{\| \bar{\mathbf{w}}_k \|_2^2}}$, $\mathbf{w}_k = \eta_k \bar{\mathbf{w}}_k$, $\forall k \in \mathcal{K}$.
12: **end while**
13: $\mathbf{W}'_s = [\mathbf{w}_{s,1}, ..., \mathbf{w}_{s,K}]$,
14: $\mathbf{W}_s = \min(\sqrt{\frac{P_s}{\| \mathbf{W}'_s \|_F^2}}, 1) \cdot \mathbf{W}'_s$, $\forall s \in \mathcal{S}$.
15: **Output:** $\{\mathbf{W}_s\}_{\forall s}$.

Leveraging (32), (27), and **Proposition 3**, we propose **MS-JoMWMMSE**, which is summarized in **Algorithm 1**. The computational complexity primarily stems from Step 10 and is $\mathcal{O}\left(I_{\max} K (S^3 N_{\mathrm{T}}^3) \right)$. $I_{\max}$ and χ denote the iteration number and the rate difference for termination, respectively. Similarly, based on [14] and Appendix A, a corresponding algorithm can also be proposed for the WMMSE problem in Section IV-A, which we refer to as **MS-JoWMMSE**.

As stated in Section III-B, the distribution of the phase error $\varphi_{s,k}$ depends on the estimation method. Without loss of generality, we adopt the modeling approach used in [4], [14], where $\varphi_{s,k} = \mathrm{e}^{j \varrho_{s,k}}$ and $\varrho_{s,k} \sim \mathcal{N}(0, \zeta_{s,k}^2)$. In this case, $\bar{\varphi}_{s,k} = \mathrm{e}^{-\frac{\zeta_{s,k}^2}{2}}$. Accurate statistical CSI and stable inter-satellite links are essential. If CSI—especially angle data—is inaccurate, error models can support robust algorithms, and link stability can be improved through better satellite selection and communication techniques. Moreover, joint user scheduling and precoding using multi-satellite statistical CSI can further boost transmission performance.

V. Numerical Results

We use the QuaDRiGa channel simulator to generate the scenario and radio channel parameters [29]. In particular, the 'QuaDRiGa_NTN_Urban_LOS' model is implemented to generate the parameters in (1). This simulator, with appropriately calibrated parameters, is aligned with the channel model considered in this work and the Third Generation Partnership Project specifications [17], [29]. Other simulation parameters are provided in Table I. Although the radius of the cooperative transmission coverage area is set at 800 km, it does not affect the performance conclusions of the designed method. Monte

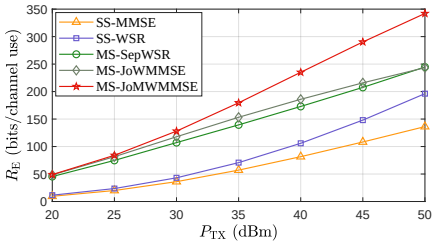

Fig. 3. Average sum rate vs P_{TX} (performance comparison under different SNRs), $\zeta_{s,k}^2 = 0.5$.

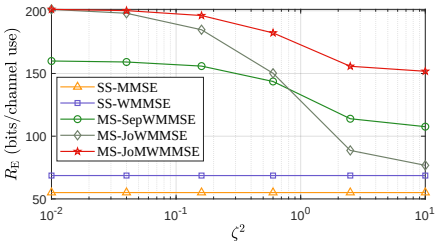

Fig. 4. Average sum rate vs $\zeta_{s,k}^2$ (performance comparison under different phase error variances), $\kappa_{s,k} = 25\mathrm{dB}$, $P_{\mathrm{TX}} = 35\mathrm{dBm}$.

TABLE I
SIMULATION PARAMETERS [12], [16], [17], [29], [30]

Parameter	Value
Satellites altitude	600 km
Carrier frequency	2 GHz
System bandwidth (DL)	20 MHz
Subcarrier spacing	30kHz
UT noise figure	7 dB
UT antenna temperature	290 K
Coverage radius	800 km
Number of UTs	48
Distribution of UTs	Uniform
Per-element gain of TX antennas	6dBi
Gain of RX antennas	0dBi
Constellation type	Walker-Delta
Orbital planes	28
Satellites per plane	60
Inclination (degrees)	53
Average inter-satellite distance	631km

Carlo simulations are conducted, where each run involves randomly selecting a point within the constellation's coverage area as the center. A circular region with the given coverage radius is defined, and the $S = 5$ closest satellites to the center are selected for cooperative transmission. In our simulations, we assume that the power constraints of all satellites are identical, i.e., $P_s = P_{\mathrm{TX}}, \forall s$, and set its range as $P_{\mathrm{TX}} \in [20\mathrm{dBm}, 50\mathrm{dBm}]$. This range can also simulate different link budgets resulting from various transceiver configurations. This section compares the following schemes:

- '**SS-MMSE**' and '**SS-WMMSE**': The MMSE and WMMSE precoding performed based on the expectation of the compensated channel, with service provided by single satellite [26].
- '**MS-SepWMMSE**': WMMSE precoding is performed separately on multiple satellites based on the expectation of the compensated channels.
- '**MS-JoWMMSE**' and '**MS-JoMWMMSE**': The proposed WMMSE- and MWMMSE-based method in Section IV-A and IV-D with $I_{\max} = 10$ and $\chi = 0.001$.

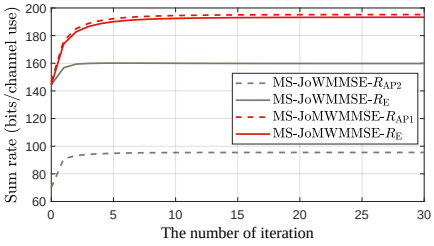

Fig. 5. Convergence of the proposed method, $\zeta_{s,k}^2 = 0.5$, $P_{\mathrm{TX}} = 35\mathrm{dBm}$.

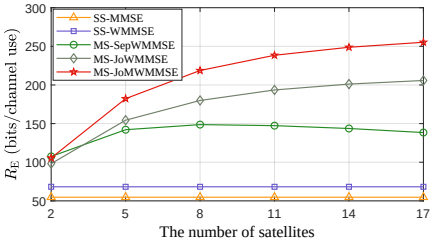

Fig. 6. Average sum rate vs the number of cooperative satellites, $\zeta_{s,k}^2 = 0.5$, $P_{\mathrm{TX}} = 35\mathrm{dBm}$.

The comparison of average sum rate $R_{\mathrm{E}} = \sum_{k\in\mathcal{K}} \mathbb{E}\{R_k\}$ performances with $N_{\mathrm{v}} = N_{\mathrm{h}} = 10$ and $\zeta_{s,k}^2 = 0.5$ are shown in Fig. 3. It can be observed that the sum rate of MS-JoMWMMSE is higher than MS-JoWMMSE, and the gain becomes larger as the SNR increases, while multi-satellite precoding can significantly outperform single-satellite precoding. Fig. 4 illustrates the impact of phase errors on performance. It can be observed that the difference between schemes MS-JoMWMMSE and MS-JoWMMSE widens as the phase error increases, which is consistent with **Remark 2**. Fig. 5 shows the evolution of R_{E} along with two sum-rate approximations over the iterations: $R_{\mathrm{AP1}} = \sum_{k\in\mathcal{K}} \bar{R}_k$ and $R_{\mathrm{AP2}} = \sum_{k\in\mathcal{K}} \tilde{R}_k$, where $\tilde{R}_k = \log_2\left(e_k^{-1}\right)$. These are sum rate approximations adopted by MS-JoMWMMSE and MS-JoWMMSE, respectively. It is evident that R_{AP2} deviates further from R_{E}, while R_{AP1} is closer to R_{E}—this is one of the reasons why **Proposition 1** and **2** demonstrate the superiority of MS-JoMWMMSE over MS-JoWMMSE. Finally, Fig. 6 shows the effect of increasing the number of satellites on performance. Notably, since MS-SepWMMSE does not suppress interference cooperatively, increasing the number of satellites may introduce more interference, ultimately leading to performance degradation.

VI. CONCLUSION

This paper investigated the distributed precoding design for multi-satellite cooperative transmission. We first conducted a detailed analysis of the transceiver process, examining the effects of delay and Doppler compensation errors and emphasizing the independence of inter-satellite interference signals. Then, we formulated the WSR problem that considers both sCSI and compensation errors. While similar problems are often recast as a WMMSE problem, we demonstrated that such problem is not equivalent to the WSR problem. Accordingly, we proposed an equivalent MWMMSE problem, investigated a low-complexity matrix decomposition method, and proposed a

$$f = \sum_{k=1}^{K} \beta_k - \beta_k \log_2(e_k^{-1}) = \sum_{k=1}^{K} \beta_k - \beta_k \log_2 \left(1 + \frac{\mathbf{w}_k^H \mathbb{E}\{\bar{\mathbf{h}}_k^*\}\mathbb{E}\{\bar{\mathbf{h}}_k^T\}\mathbf{w}_k}{\sum_{i\neq k} \mathbf{w}_i^H \tilde{\mathbf{\Omega}}_k \mathbf{w}_i + \mathbf{w}_k^H \mathbf{\Omega}_k \mathbf{w}_k - \mathbf{w}_k^H \mathbb{E}\{\bar{\mathbf{h}}_k^*\}\mathbb{E}\{\bar{\mathbf{h}}_k^T\}\mathbf{w}_k + \sigma_k^2}\right). \tag{40}$$

solution algorithm. Simulation results demonstrated the effectiveness and robustness of the proposed method under representative practical scenarios.

APPENDIX A
PROOF OF PROPOSITION 1

For given $\mathbf{W}$, it can be proved that the optimal receiver is

$$a_k^\star = \frac{\mathbb{E}\{\bar{\mathbf{h}}_k^T\}\mathbf{w}_k}{\left(\sum_{i\neq k} \mathbf{w}_i^H \tilde{\mathbf{\Omega}}_k \mathbf{w}_i + \mathbf{w}_k^H \mathbf{\Omega}_k \mathbf{w}_k\right) + \sigma_k^2}. \tag{39}$$

Note that this optimal expression is independent of the value of $\mathbf{u}$. With the optimal receiver and given $\mathbf{W}$, the optimal weight is $u_k^\star = e_k^{-1}$. By successively substituting the optimal expressions of $\mathbf{u}^\star$ and $\mathbf{a}^\star$ into the objective function of $(\mathcal{P}_2)$, we obtain the function that depends only on $\mathbf{W}$, which is expressed as (40). Although the last term in the equation is similar to the sum rate expression in (21), it is identical to the sum rate expression in (21) only when $\mathbb{E}\{\bar{\mathbf{h}}_k^*\}\mathbb{E}\{\bar{\mathbf{h}}_k^T\} = \mathbb{E}\{\bar{\mathbf{h}}_k^*\bar{\mathbf{h}}_k^T\}, \forall s \in \mathcal{S}$, which is equivalent to $\mathbb{E}\{\bar{\mathbf{h}}_{s,k}^*\mathbf{h}_{s,k}^T\} = \mathbb{E}\{\bar{\mathbf{h}}_{s,k}^*\}\mathbb{E}\{\mathbf{h}_{s,k}^T\},\ \forall s \in \mathcal{S}, k \in \mathcal{K}$. This concludes the proof.

ACKNOWLEDGEMENT

This work was supported in part by the National Key R&D Program of China (Grant 2023YFB2904703) and in part by the Luxembourg National Research Fund (FNR) (Grant reference INTER/MOBILITY/2023/IS/18014377/MCR).

REFERENCES

[1] K. Ntontin, E. Lagunas, J. Querol, J. u. Rehman *et al.*, "A vision, survey, and roadmap toward space communications in the 6G and beyond era," *Proc. IEEE*, pp. 1–37, 2025.

[2] M. Á. Vázquez, M. R. B. Shankar, C. I. Kourogiorgas, P.-D. Arapoglou *et al.*, "Precoding, scheduling, and link adaptation in mobile interactive multibeam satellite systems," *IEEE J. Sel. Areas Commun.*, vol. 36, no. 5, pp. 971–980, 2018.

[3] X. Zhang, J. Wang, C. Jiang, C. Yan *et al.*, "Robust beamforming for multibeam satellite communication in the face of phase perturbations," *IEEE Trans. Veh. Technol.*, vol. 68, no. 3, pp. 3043–3047, 2019.

[4] W. Wang, L. Gao, R. Ding, J. Lei *et al.*, "Resource efficiency optimization for robust beamforming in multi-beam satellite communications," *IEEE Trans. Veh. Technol.*, vol. 70, no. 7, pp. 6958–6968, 2021.

[5] L. You, K.-X. Li, J. Wang, X. Gao *et al.*, "Massive MIMO transmission for LEO satellite communications," *IEEE J. Sel. Areas Commun.*, vol. 38, no. 8, pp. 1851–1865, 2020.

[6] S. Wu, Y. Wang, G. Sun, L. You *et al.*, "Energy and computational efficient precoding for LEO satellite communications," in *Proc. IEEE Glob. Commun. Conf. (GLOBECOM)*, Dec. 2023, pp. 1872–1877.

[7] M. Y. Abdelsadek, G. K. Kurt, and H. Yanikomeroglu, "Distributed massive MIMO for LEO satellite networks," *IEEE Open J. Commun. Soc.*, vol. 3, pp. 2162–2177, Nov. 2022.

[8] M. Röper, B. Matthiesen, D. Wübben, P. Popovski *et al.*, "Beamspace MIMO for satellite swarms," in *Proc. IEEE Wireless Commun. Netw. Conf. (WCNC)*, Apr. 2022, pp. 1307–1312.

[9] M. Y. Abdelsadek, G. Karabulut-Kurt, H. Yanikomeroglu, P. Hu *et al.*, "Broadband connectivity for handheld devices via LEO satellites: Is distributed massive MIMO the answer?" *IEEE Open J. Commun. Soc.*, vol. 4, pp. 713–726, Mar. 2023.

[10] X. Zhang, S. Sun, M. Tao, Q. Huang *et al.*, "Multi-satellite cooperative networks: Joint hybrid beamforming and user scheduling design," *IEEE Trans. Wireless Commun.*, pp. 7938 – 7952, Jul. 2024.

[11] Z. Xu, Y. Gao, G. Chen, R. Fernandez *et al.*, "Enhancement of satellite-to-phone link budget: An approach using distributed beamforming," *IEEE Veh. Technol. Mag.*, vol. 18, no. 4, pp. 85–93, Oct. 2023.

[12] Z. Xiang, X. Gao, K.-X. Li, and X.-G. Xia, "Massive MIMO downlink transmission for multiple LEO satellite communication," *IEEE Trans. Commun.*, vol. 72, no. 6, pp. 3352–3364, Jun. 2024.

[13] V. N. Ha, D. H. N. Nguyen, J. C.-M. Duncan, J. L. Gonzalez-Rios *et al.*, "User-centric beam selection and precoding design for coordinated multiple-satellite systems," in *Proc. IEEE 35th Int. Symp. Personal, Indoor and Mobile Radio Commun. (PIMRC)*, Sept. 2024, pp. 1–6.

[14] X. Chen and Z. Luo, "Asynchronous interference mitigation for LEO multi-satellite cooperative systems," *IEEE Trans. Wireless Commun.*, vol. 23, no. 10, pp. 14 956–14 971, Oct. 2024.

[15] ——, "Cooperative WMMSE precoding for asynchronous LEO multi-satellite communications," in *Proc. IEEE Int. Conf. Commun. Workshops (ICC Workshops)*, Jun. 2024, pp. 1691–1696.

[16] 3GPP, "TR 38.821 v16.2.0: Solutions for NR to support non-terrestrial networks (NTN)," 3GPP, Tech. Rep. TR 38.821 V16.2.0, Mar. 2023.

[17] ——, "TR 38.811 v15.4.0: Study on new radio (NR) to support non-terrestrial networks," 3GPP, Tech. Rep. TR 38.811 V15.4.0, Sep. 2020.

[18] L. Bai, C.-X. Wang, G. Goussetis, S. Wu *et al.*, "Channel modeling for satellite communication channels at Q-band in high latitude," *IEEE Access*, vol. 7, pp. 137 691–137 703, 2019.

[19] S. Wu, G. Sun, Y. Wang, L. You *et al.*, "Low-complexity user scheduling for LEO satellite communications," *IET Commun.*, vol. 17, no. 12, pp. 1368–1383, May 2023.

[20] Y. Wang, H. Hou, X. Yi, W. Wang *et al.*, "Towards unified AI models for MU-MIMO communications: A tensor equivariance framework," *IEEE Trans. Wireless Commun.*, Jun. 2025, Early Access.

[21] W. Wang, Y. Tong, L. Li, A.-A. Lu *et al.*, "Near optimal timing and frequency offset estimation for 5G integrated LEO satellite communication system," *IEEE Access*, vol. 7, pp. 113 298–113 310, 2019.

[22] M. Yuan, H. Wang, H. Yin, and D. He, "Alternating optimization based hybrid transceiver designs for wideband millimeter-wave massive multiuser MIMO-OFDM systems," *IEEE Trans. Wireless Commun.*, vol. 22, no. 12, pp. 9201–9217, Dec. 2023.

[23] E. Björnson, M. Bengtsson, and B. Ottersten, "Optimal multiuser transmit beamforming: A difficult problem with a simple solution structure [lecture notes]," *IEEE Signal Process. Mag.*, vol. 31, no. 4, pp. 142–148, Jul. 2014.

[24] M. Bengtsson and B. Ottersten, "Optimal downlink beamforming using semidefinite optimization," in *Proc. 37th Annual Allerton Conference on Communication, Control, and Computing*, Sep. 1999, pp. 987–996, invited paper.

[25] ——, "Optimal and suboptimal transmit beamforming," in *Handbook of Antennas in Wireless Communications*, L. C. Godara, Ed. CRC Press, Aug. 2001.

[26] S. S. Christensen, R. Agarwal, E. De Carvalho, and J. M. Cioffi, "Weighted sum-rate maximization using weighted MMSE for MIMO-BC beamforming design," *IEEE Trans. Wireless Commun.*, vol. 7, no. 12, pp. 4792–4799, Dec. 2008.

[27] Q. Shi, M. Razaviyayn, Z.-Q. Luo, and C. He, "An iteratively weighted MMSE approach to distributed sum-utility maximization for a MIMO interfering broadcast channel," *IEEE Trans. Signal Process.*, vol. 59, no. 9, pp. 4331–4340, Sept. 2011.

[28] M. Joham, K. Kusume, M. H. Gzara, W. Utschick *et al.*, "Transmit wiener filter for the downlink of TDDDS-CDMA systems," in *Proc. IEEE 7th Int. Symp. Spread Spectrum Techniques and Applications*, vol. 1, 2002, pp. 9–13.

[29] S. Jaeckel, L. Raschkowski, and L. Thieley, "A 5G-NR satellite extension for the QuaDRiGa channel model," in *Proc. Joint Eur. Conf. Netw. Commun. & 6G Summit (EuCNC/6G Summit)*, 2022, pp. 142–147.

[30] "Federal communications commission; amendment to pending application for the SpaceX Gen2 NGSO satellite system," FCC, Washington, D.C., Tech. Rep. File No. SAT-AMD-2021, August 2021, available: https://fcc.report/IBFS/SAT-AMD-20210818-00105/12943361.pdf.